Research article

SURFACE and INTERFACE ANALYSIS

Received: 10 October 2016 Revised: 14 December 2016 Accepted: 2 January 2017 Published online in Wiley Online Library

(wileyonlinelibrary.com) DOI 10.1002/sia.6209

The effect of interface electrostatic interaction based on acid–base theory on friction behavior

Li Qiang,[a] Zhongyue Cao,[a,b] Jing Shi,[a,b] Yan Zhou,[a] Aimin Liang[a]* and Junyan Zhang[a]*

Fluorine-containing amorphous carbon films [fluoring-containing diamond-like carbon (F-DLC)] were fabricated on Si wafer by direct current plasma enhanced chemical vapor deposition (dc-PECVD) technique using CF_4 and Ar as gas sources, confirmed by XPS and Raman analyses. The friction tests were carried out on a rotating ball-on-disk apparatus in high vacuum atmosphere ($\leq 5.0 \times 10^{-4}$ Pa) at the load of 0.5 N selecting glass (mainly containing silicon–oxygen tetrahedron structure) and Al_2O_3 with the same hardness and surface roughness as the counterpart balls. The results indicate that glass/F-DLC results in lower friction coefficient of 0.14 than that of the Al_2O_3/F-DLC (0.20). At the same time, no wear was occurred, and the transfer layer was not formed on the counterpart ball for glass/F-DLC, while the wear of Al_2O_3/F-DLC is slightly larger than that of glass/F-DLC. However, just like the glass ball, there is no formation of transfer layer on the Al_2O_3 ball surface. Furthermore, the chemical state of fluorine in the film after friction, which mainly existed in the form of the C–CF and C–F bonds, did not change compared with the F-DLC film, while the fluorine content has changed significantly. As a result, it is assumed that interface electrostatic interaction based on acid–base theory plays an extremely important role in the process of friction. Copyright © 2017 John Wiley & Sons, Ltd.

Keywords: F-DLC film; friction surface; electrostatic interaction; friction

Introduction

Much attention has been paid to the investigation on the tribological behaviors of diamond-like carbon (DLC) films considered as novel solid lubricant with low friction and outstanding wear resistance.[1,2] However, the tribological behaviors of DLC films vary significantly in terms of different experimental conditions. Understanding the different tribological behaviors of DLC films under different conditions is very important to bring DLC films to more applications to meet actual requirements. The existing studies have shown that, besides the intrinsic natures, the tribological behaviors of DLC films could be affected heavily by extrinsic factors, such as roughness, surface, or interfacial physical and chemical characteristics of the counterpart surface.[3] Among these factors, the adhesion or chemical interaction between the sliding surfaces is considered to be the most decisive one, especially for atomically smooth surfaces.[4,5]

Adhesion or chemical interaction mainly includes σ covalent bonds, π–π^* interaction, electrostatic forces, and van der Waals forces in turn according to the strength. σ covalent bonds may form between hydrogen-free DLC films because of the presence of dangling bonds, particularly under ultra-high vacuum or inert gas atmosphere, leading to high friction coefficient when sliding against each other. For instance, the friction coefficient of tetrahedral carbon (ta-C) films reaches up to 0.65.[6] Hydrogen-free amorphous carbon (a-C) can easily form strong covalent bonds in dry N_2 atmosphere, and the friction coefficient can reach as high as 0.42.[7] When the counterfaces with certain sp^2 hybridization graphitic phase slide against each other, for example, sp^2 hybridization dominated DLC films and glassy carbon, π–π^* interaction occurs at the interface, which is analogous to crystalline graphite.[8] Compared with other adhesion or chemical interactions, σ covalent bonds or π–π^* interaction dominate the friction coefficient for hydrogen free DLC films in ultra-high vacuum or inert gas atmosphere, resulting in high friction coefficient.

In order to eliminate the dangling bonds of DLC films to reduce the effect of σ covalent bonds or π–π^* interaction to lower friction, hydrogen is generally introduced into DLC films, named hydrogenated DLC films. The incorporation of hydrogen into DLC films not only terminates dangling bond but also eliminates π–π^* interaction at the sliding DLC interfaces because of the presence of hydrogen at film surface.[8,9] In this case, the surface of hydrogenated DLC film could be considered as polar surface because of the polarity of C–H bond; the surface of counterpart materials is generally also considered as polar surface because most of the time they are not pure homogeneity in chemistry. Therefore, compared with van der Waals force, electrostatic forces are becoming the most important factor at the interface of hydrogenated DLC film and counterpart, particularly, when F, more electronegative, is introduced into hydrogenated DLC films to reduce the surface energy.[10]

Sen *et al.* exerted first principle method predicating the interaction of two fluorine-containing DLC (F-DLC) surfaces and

* *Correspondence to: Junyan Zhang, State Key Laboratory of Solid Lubrication, Lanzhou Institute of Chemical Physics, Chinese Academy of Sciences, Lanzhou 730000, China.*
E-mail: zhangjunyan@licp.cas.cn; Liangaimin55@aliyun.com

a *State Key Laboratory of Solid Lubrication, Lanzhou Institute of Chemical Physics, Chinese Academy of Sciences, Lanzhou 730000, China*

b *University of Chinese Academy of Sciences, Beijing 100049, China*

found that there is stronger repulsive force than that in the case of two H-DLC films.[11] The σ bond breaking of C–H, C–C and the formation of AlF_3 account for high friction coefficient, while the repulsive force between F-terminated transfer film and the fluorinated DLC surface results in low steady friction coefficient.[12,13] Hence, to probe the adhesion or chemical interaction of the DLC films and counterpart is of help to understand the tribological behaviors of DLC films and to guide the design of the DLC film with certain surface characteristic so as inversely to control or adjust the tribological behaviors of DLC films as solid lubricant. Here, we propose a new perspective based on acid–base theory to study the adhesion or chemical interaction of DLC film, to investigate, and to reveal the interfacial interaction as well as tribological behaviors of DLC film and counterpart.

Fluorine-containing DLC film could be thought as Lewis base according to the nature of C–F bond. We choose two representative ceramic balls as counterpart to F-DLC film, glass [$Na_2O{\cdot}(SiO_2)_n$] and Al_2O_3, which could be considered as Lewis base and Lewis acid, respectively, according to acid–base theory that defines Lewis base and Lewis acid with nucleophilicity and electrophilicity. Glass, consisting of bridging and none-bridging oxygen,[14] can be considered to be nucleophilic. Al_2O_3 surface, terminated by Al atoms[15,16], is eletrophilid. When glass and Al_2O_3 slide against F-DLC films, there will be interfacial nucleophilic or electrophilic electrostatic interaction, which makes the friction coefficient of glass/F-DLC lower than that of Al_2O_3/F-DLC due to the base–base electrostatic repulsive force for glass/F-DLC and the acid–base electrostatic attractive force for Al_2O_3/F-DLC.

Experimental procedure

Films deposition

Direct current plasma-enhanced chemical vapor deposition was used to fabricate F-DLC films using CF_4 and Ar as gas sources. Si (n-100) substrates were ultrasonically cleaned in acetone and ethanol in sequence and then placed on the cathode electrode. Prior to deposition, the substrates were in suit sputter cleaned by argon discharge with 300 sccm gas flow at 5.8 Pa working pressure and the bias voltage of −800 V for 30 min. CF_4 and Ar gas with high purity were introduced into the chamber as precursor. The specific deposition conditions of fluorine-containing amorphous carbon films were deposited at the following parameters: base pressure = 4.7 Pa, bias voltage = −800 V, deposition time = 60 min.

Sample characterization

The thickness of the film was measured by scanning electron microscope (SEM, JSM-5600LV). Surface morphology and roughness were analyzed by atomic force microscope (AFM; AIST-NT, SmartSPM, USA). The mechanical properties were measured by nanoindenter (Nano inderter II, MTS co. Ltd of America) with a maximum indentation depth of 80 nm in order to avoid the influence of substrate. Raman spectrum was obtained by using a Jobin Yvon T64000 Raman spectroscope (HORIBA Scientific,France) at the excitation wavelength of the 514 nm Ar laser line and with a spot size of 5 μm. The spectral resolution was less than 1 cm^{-1}. The chemical bonding and composition of the deposited films were assessed by X-ray photoelectron spectroscope (XPS) using a Kratos AXIS Ultra^{DLD} instrument (Shimadzu/Kritos company, Japan) operated with an Al target X-ray source (Al anode operated at maximum 600 W).

The tribological tests were conducted on self-developed high vacuum friction and wear rotation tester selecting two kinds of ceramic balls as counterparts. One was glass and the other was corundum with the similar hardness and surface roughness in order to avoid its influence. The structure of the glass balls (ϕ = 5 mm, Ra ≤ 12 nm, Moh's hardness = 7) mainly containing silicon–oxygen tetrahedron, which could be indicated as $Na_2O{\cdot}(SiO_2)_n$, and here, it was selected as Lewis base for its nucleophilicity of the bridging and none-bridging oxygen it contains. All mentioned Na_2SiO_3 or glass ball refers to silicon–oxygen tetrahedron ball in this paper. The structure of the corundum balls of α-Al_2O_3 (ϕ = 5 mm, Ra ≤ 16 nm, Moh's hardness = 9) was selected as Lewis acid for its electrophilicity of Al^+ ions terminating the surface. The parameters of tribological tests were as follows: the frictional load = 0.5 N, the speed = 30 r/min, the radius = 5 mm, and the testing time = 7 min. The friction tests were carried out utilizing a ball-on-disk apparatus in high vacuum atmosphere (≤5.0×10^{-4} Pa) at least three times to ensure the repeatability. After testing, the 3D morphology of wear scar of film was observed by a surface three-dimensional profiler, and the surface morphology of wear tracks of film and counterparts was observed by an OLYMPUS optical microscope (OLYMPUS Company, Japan).

Results and discussion

Thickness, surface roughness, and mechanical properties

The field emission SEM (JSM-6701F) was used to determine the thickness of F-DLC film by measuring the cross section of the film, and the thickness of the film is about 834 nm (Fig. 1(a)). The surface roughness of film is less than 1 nm (0.794 nm, as shown in Fig. 1(b)). Therefore, the impact of the surface roughness on the friction of F-DLC film could be neglectable. Figure 1(c) shows the hardness and elastic modulus of the film. The hardness and elastic modulus of the film is 4.36 GPa and 38.3 GPa, respectively. The specific data of film are summarized in Table 1.

Raman and XPS analysis

The Raman measurement is a fast and nondestructive method for the characterization of carbon materials. Figure 2(a) shows the Raman spectrum for the F-DLC film deposited in this experiment. A broad asymmetric Raman bond, which represents the typical features of the conventional DLC films, could be observed in the wave number range of 800–2000 cm^{-1}. The Raman spectrum can be deconvoluted into two Gaussian peaks, the peak at 1538 cm^{-1} corresponds to the *G* peak, ascribed to the optical zone center vibration (E_{2g} mode) of all pairs of sp^2 bonding in both aromatic rings and olefinic chains, and the other is the shoulder peak around 1349 cm^{-1}, corresponding to the *D* peak, originated from the breathing vibration of sp^2 bonding only in sixfold rings.[17] Generally, the peak intensities ratio (I_D/I_G) is proportional to the number of rings per cluster, but contrary to the fraction of chain groups.[18] The Raman spectrum with only *G* and *D* peaks demonstrates diamond-like structure of the F-DLC film.[19] The ratio of peak intensities (I_D/I_G) is as low as 0.5, predicting that some chain-like structure of olefinic compounds (sp^3 sites) form in the DLC matrix.[20]

To investigate the surface composition and bonding state of the F-DLC film, XPS spectra were obtained. The F content for the film is 5.84 at.%. To explore the surface bonding type, the C1s XPS spectra of the as-deposited F-DLC film is presented in Fig. 2(b), which can be deconvolved by Gaussian fitting into four sub-peaks: 284.4,

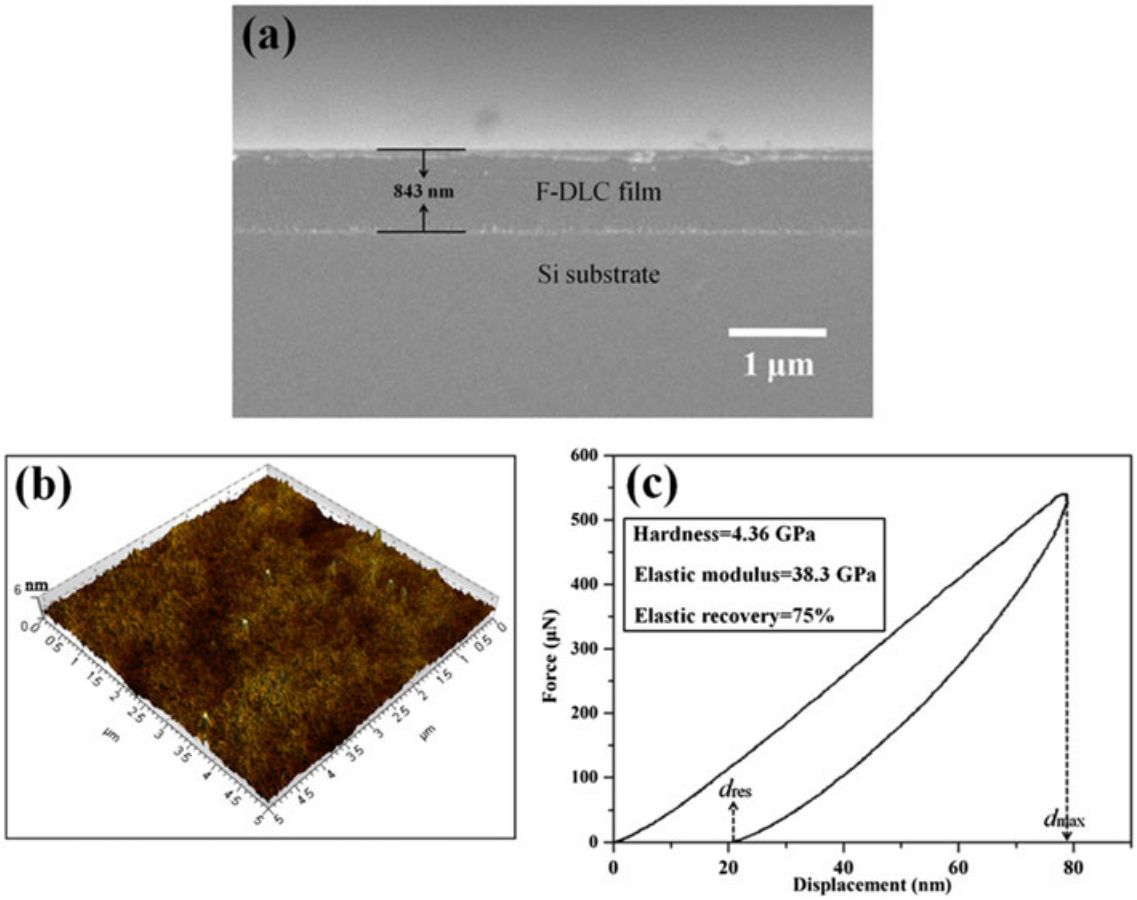

Figure 1. (a) Thickness, (b) surface roughness, and (c) mechanical properties of the film. F-DLC, fluorine-containing diamond-like carbon. [Colour figure can be viewed at wileyonlinelibrary.com]

Table 1. Thickness, surface roughness, and mechanical data of F-DLC film

	Thickness	Surface roughness	Hardness	Elastic modulus
	(nm)	(nm)	(GPa)	(GPa)
F-DLC film	834	0.794	4.36	38.30

F-DLC, fluorine-containing diamond-like carbon.

285.2, 286.6, and 289.1 eV, representing sp2-C, sp3-C, C–CF, and C–F, respectively.[21] These results show that the incorporation of F element produces the chemical bonding of fluorocarbon in the DLC film, thus terminating the surface carbon dangling bonds. Combining Raman spectrum with XPS results, it can be seen that the film prepared by this experiment is the typical amorphous F-DLC film.

Tribological behavior

The friction coefficients for glass/F-DLC and Al_2O_3/F-DLC were investigated under the loads of 0.5 N as depicted in Fig. 3. As shown in Fig. 3(a), the friction coefficient of glass/F-DLC stabilizes at 0.14, lower than that of Al_2O_3/F-DLC (μ = 0.2). Figure 3(b) and Fig. 3(c) show wear tracks micrograph and corresponding cross-section profiles of the of F-DLC films against Al_2O_3 and glass, respectively. It can be seen that the wear track is superfine, and nano-level wear depth is imperceptible. Moreover, optical microscope (OLYMPUS STM6) was adopted to observe the wear tracks of the film and wear scars of counterpart balls to obtain further comprehension of the friction experiments. Figure 4 shows the typical optical micrograph of the wear tracks on the film and wear scars on the counterpart balls. As shown in Fig. 4(a) and (c), for the glass/F-DLC film, almost no wear debris was found around the wear tracks, and there is also no transfer layer on its corresponding counterpart ball, which implies no wear occurred, and transfer layers were not formed on the counterpart ball. Meanwhile, for Al_2O_3/F-DLC film as shown in Fig. 4(b) and (d), a small amount of wear debris could be found along the wear tracks, and negligible amount of materials transfer, but which did not form a complete transfer layer, occurred on the Al_2O_3 ball, which demonstrates that the wear of F-DLC film sliding against Al_2O_3 ball is slightly larger than that of F-DLC film tested against glass. However, just like the glass ball, there is no formation of transfer layer on the surface of Al_2O_3 ball.

XPS analysis of wear tracks

The chemical state of the wear tracks of F-DLC film tested against glass and Al_2O_3 ball was performed by XPS. Figure 5 presents the full spectrum, F1s, C1s high-resolution XPS spectra of the wear tracks of glass/F-DLC film and Al_2O_3/F-DLC film. As shown in Fig. 5(a), three major peaks around 284.5, 533.4, and 688 eV were observed for F-DLC film and glass/F-DLC film. The peak around 284.5 eV, representing the typical binding energy of the DLC film, is assigned to C1s peak, and the peak about 533.4 and 688 eV are

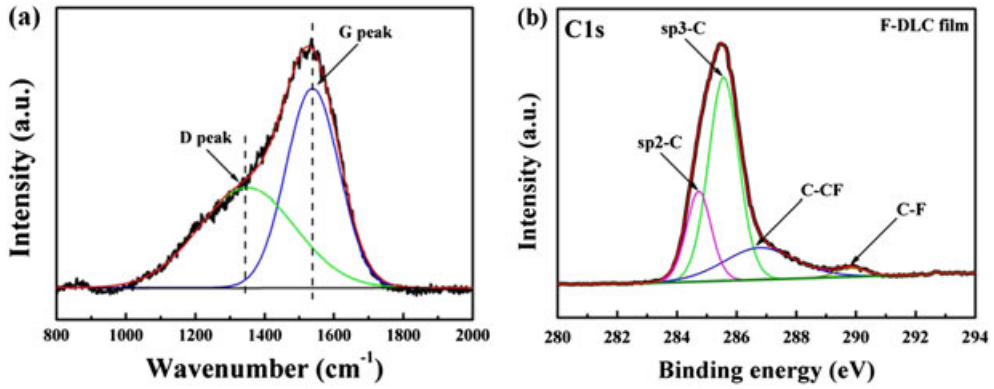

Figure 2. (a) Raman spectrum and (b) deconvolution of XPS C1s spectrum of the film. F-DLC, fluorine-containing diamond-like carbon. [Colour figure can be viewed at wileyonlinelibrary.com]

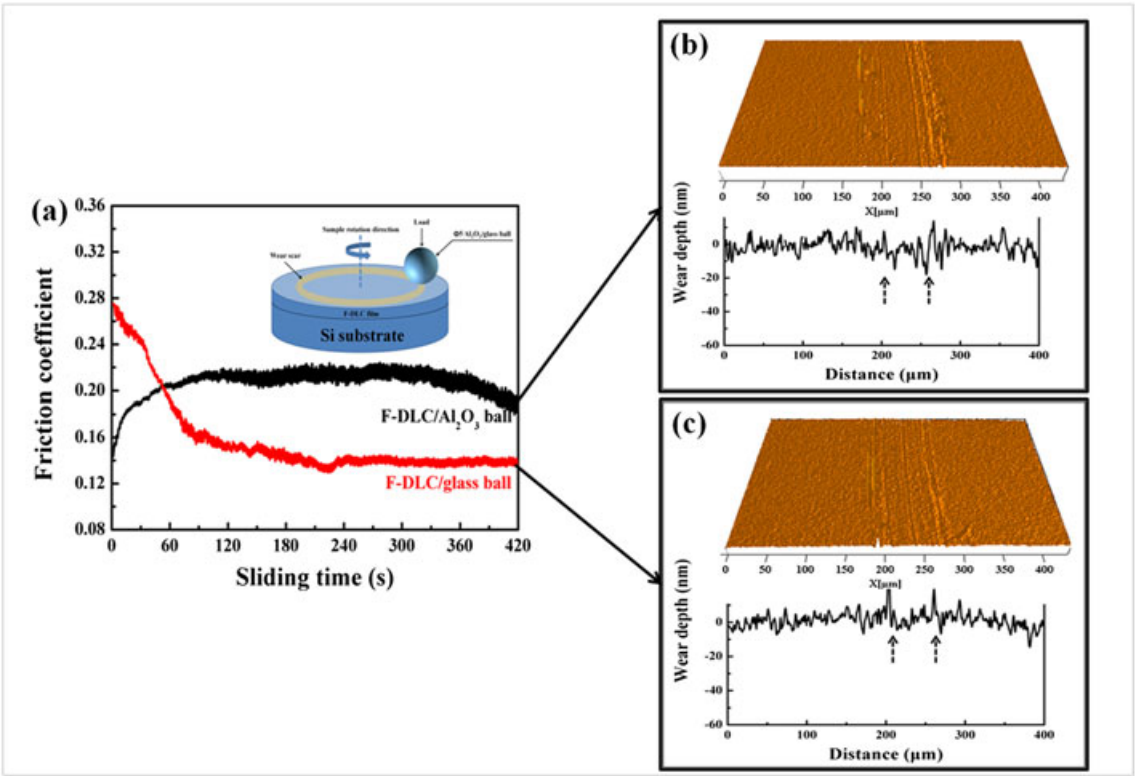

Figure 3. (a) The friction coefficients for glass/F-DLC and Al_2O_3/F-DLC at load of 0.5 N, and a schematic of the test geometry is shown in inset. Wear tracks micrograph and corresponding cross-section profiles of films sliding against Al_2O_3 and glass are shown in (b) and (c), respectively. F-DLC, fluorine-containing diamond-like carbon. [Colour figure can be viewed at wileyonlinelibrary.com]

assigned to O1s and F1s peak. The detected O1s peak might be attributed to the contamination when the film is exposed to the air after friction. However, for Al_2O_3/F-DLC film, it should be noted that the F1s peak is so small that it hardly can be discerned, which is assigned to the low fluorine concentration for the wear tracks of Al_2O_3/DLC film. XPS F1s peak shows that in Fig. 5(b), the highest relative intensity of F1s peak could be observed for the F-DLC film, representing the highest fluorine content (5.84 at.%), which is slightly higher than that of the wear tracks of glass/F-DLC film (fluorine content is 3.99 at.%). However, the lowest relative intensity of F1s peak could be found for the wear tracks of Al_2O_3/F-DLC film, implying the lowest F concentration (0.24 at.%) on the wear track for Al_2O_3/F-DLC film. As shown in Fig. 5(c) and (d), the chemical state of fluorine in the film after friction, which mainly existed in the form of the C–CF and C–F bonds, did not change compared with the F-DLC film, while the fluorine content has changed significantly. The decrease of fluorine content may be explained from the following two aspects:(i) for glass/F-DLC film, friction chemical reaction caused by friction heat and other factors caused the rupture of the C–F bond in the process of friction; and (ii) for Al_2O_3/F-DLC film, besides the aforementioned factors, the friction interface may exist the interaction force, which more easily leads to the rupture of the C–F bond and further to greatly reduce the fluorine content in the same friction conditions.

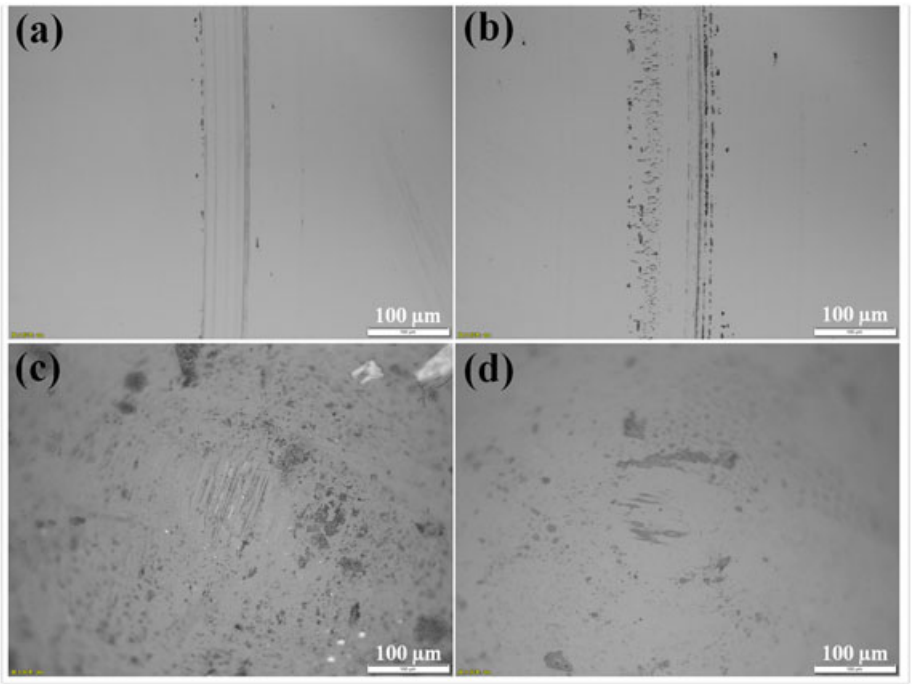

Figure 4. The surface morphology of wear tracks formed on the fluorine-containing diamond-like carbon film tested against (a) glass and (b) Al_2O_3; the corresponding wear scar image of glass ball and Al_2O_3 as shown in (c) and (d), respectively. [Colour figure can be viewed at wileyonlinelibrary.com]

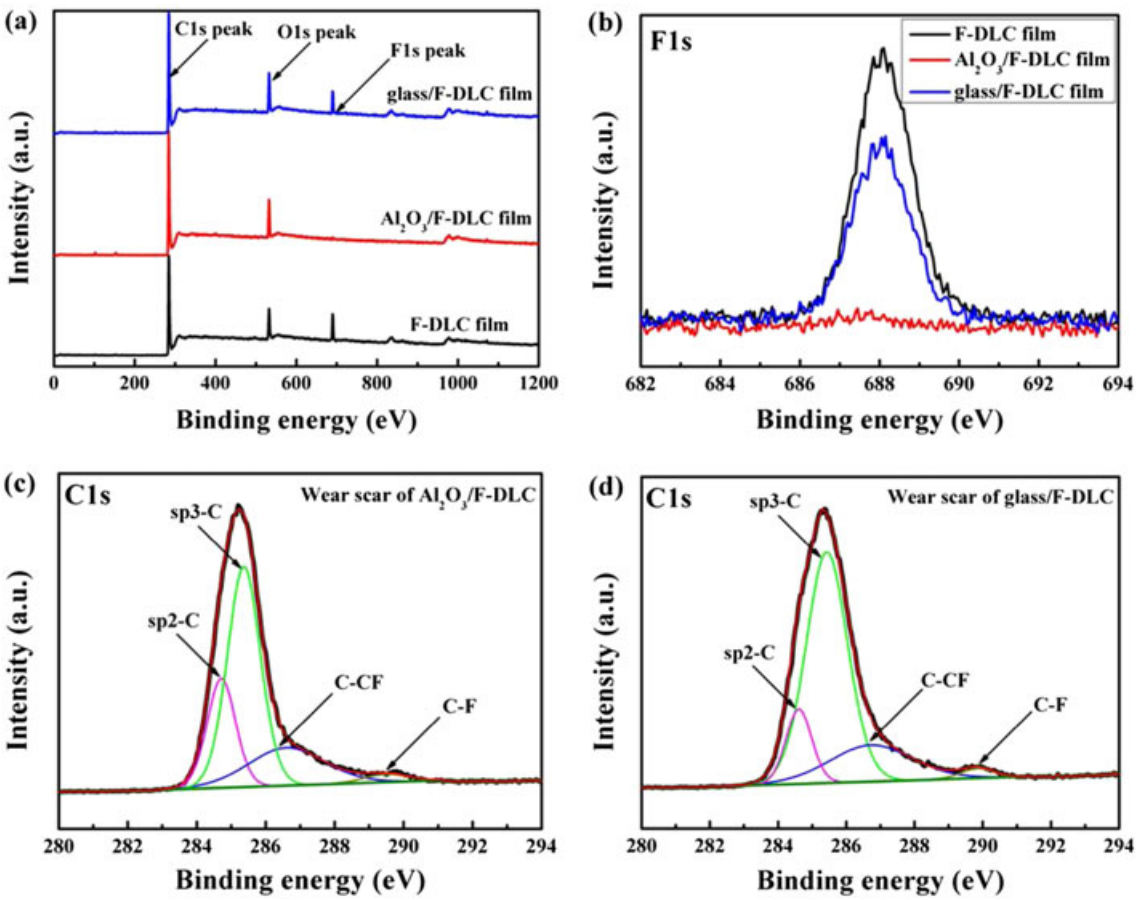

Figure 5. (a) XPS full spectrum and (b) F1s peak of the fluorine-containing diamond-like carbon (F-DLC) film and the wear tracks of glass/F-DLC and Al_2O_3/F-DLC; XPS C1s Gaussian fitting peaks of the wear tracks of (c) Al_2O_3/F-DLC and (d) glass/F-DLC. [Colour figure can be viewed at wileyonlinelibrary.com]

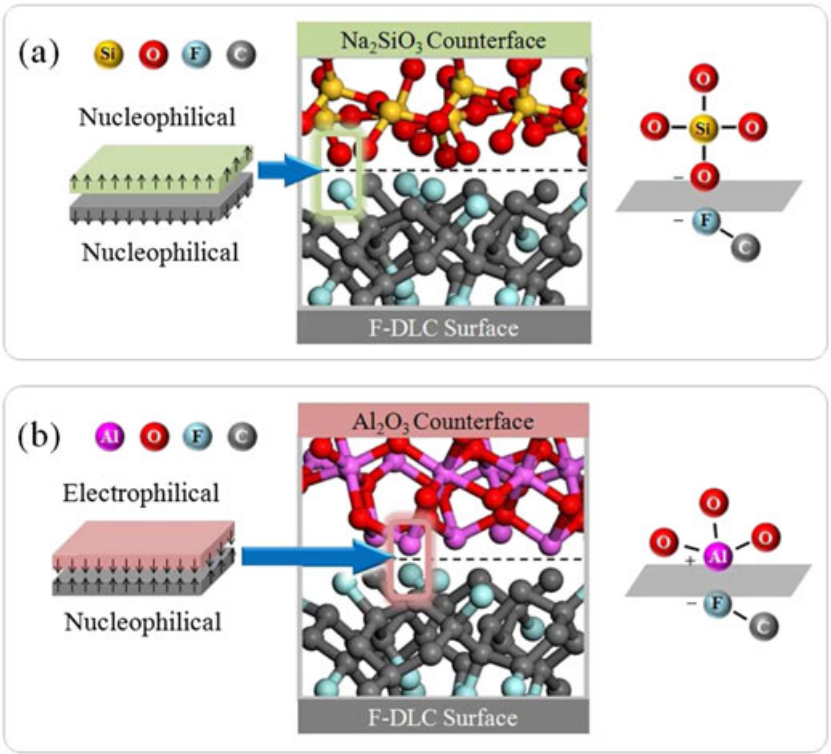

Figure 6. Schematics of the ion interactions at the interface for negatively charged O and positively charged Al interplaying with negatively charged F in (a) and (b), respectively. [Colour figure can be viewed at wileyonlinelibrary.com]

Friction mechanism analysis

Taking into account the statement mentioned earlier, on the one hand, two counterpart balls with similar hardness and surface roughness were chosen to exclude the effect of counterparts mechanical properties on friction behavior of the film; on the other hand, no obvious wear could be found on the film surface after friction, and no transfer layer could also be observed on both of the counterpart balls, thereby excluding the influence of the transfer layer on the friction interface on the friction behavior of the films. Thus, the friction and wear results point out qualitatively that interfacial nucleophilic/electrophilic electrostatic interaction plays an important role in the tribological behaviors.

Sung *et al.* gave a schematics to show the comparison of electrostatic effect between H/H terminated and F/F terminated surfaces that the later could be levitated without contact due to a larger repulsive force.[22] Quantitatively, calculations show that the vertical distance of the nearest C atoms from two F terminated surfaces corresponding to most stable adsorption energy is 5.25 Å, while that of two H terminated surfaces is 3.95 Å. In a word, there is a larger repulsive force of F/F terminated surfaces than that of H/H terminated surfaces under the same distance, of which the repulsive force is greater than zero.[23] It was also reported that the repulsive force becomes larger sharply when two F-terminated DLC surfaces are getting closer than 2.8 Å, approaching 2 eV/Å at the point of 2.5 Å.[11] The interfacial interaction mechanisms of F-DLC film with glass or Al_2O_3 could be depicted as shown in Fig. 6; the electrostatic force deriving from different interfacial interactions influences the interfacial shear strength. That is, Fig. 6(a) gives mutual repulsive force produced by the friction counterfaces with the same surface property of nucleophilicity. Glass and F-DLC films are both nucleophilic, because O atoms in glass and F atoms in the F-DLC film are the origin of nucleophilicity. The electronegativity value of C is 2.55, far lower than that of F, which is the strongest electronegative element with its value of 3.98. When C atom bonds to F atom, the electrical charge density of C is permanently shifted to pair with the outer electrons of F, thus the film surface terminated by F atoms can accumulate certain static electrical charges. For Si and O, the electronegativity value is 1.90 and 3.44, respectively. Surface bridging and none-bridging oxygen atoms in glass acquire the electrons from silicon forming dipole configuration and one electron donated by Na, which makes oxygen atoms have high electronegativity. Thus, the interaction of negatively charged O and F produces repulsive force. On the contrary, in the case with one of nucleophilicity and the other of electrophilicity, there is mutual attractive force, as shown in Fig. 6(b); the positively charged Al in the Al_2O_3 accounts for electrophilicity, and the interaction of positively charged Al and negatively charged F produces attractive force. Repulsive force reduces the shear strength of the contact, leading to weaker lateral friction force, hence, lower friction coefficient. Conversely, attractive force enhances lateral friction force, leading to higher friction coefficient.

Conclusions

Fluorine-containing amorphous carbon films (F-DLC) were fabricated on Si wafer by dc-PECVD technique using CF_4 and Ar as gas sources. Scanning electron microscope, AFM, and nanoindenter (Nano inderter II) were used to measure the thickness, surface roughness, and the hardness of film, respectively. The results show that the thickness of the film is about 834 nm. The surface roughness of the film is less than 1 nm (0.794 nm), and the hardness and elastic modulus of the film is 4.36 GPa and 38.3GPa,

respectively. Meanwhile, Raman and XPS analysis were used to investigate the surface composition and bonding states of the F-DLC film. The results confirmed that the film prepared is the typical amorphous F-DLC film, and the incorporated fluorine atoms exist mainly in the forms of the C–F and C–CF in the film. The friction tests were carried out on a rotating ball-on-disk apparatus in high vacuum atmosphere ($\leq 5.0 \times 10^{-4}$ Pa) at the load of 0.5 N selecting glass (mainly containing silicon-oxygen tetrahedron structure) and Al_2O_3 with the same hardness and surface roughness as the counterpart balls. The friction coefficient of glass/F-DLC approaches to 0.14, which is lower than that of Al_2O_3/F-DLC (0.20). On the one hand, two counterpart balls with similar hardness and surface roughness were chosen to exclude the effect of counterparts mechanical properties on friction behavior of the film; on the other hand, no obvious wear could be found on the film surface after friction, and no transfer layer could also be observed on both of the counterpart balls, thereby excluding the influence of the transfer layer on the friction behavior of the films. Thus, interfacial nucleophilic/electrophilic electrostatic interaction based on the acid–base theory could account for this phenomenon. The repulsive force of nucleophilic/nucleophilic counterparts (glass/F-DLC) reduces the shear strength of the contact and leads to lower friction coefficient. Conversely, the attractive force of nucleophilic/electrophilic counterparts (Al_2O_3/F-DLC) leads to the higher friction coefficient.

Acknowledgements

The authors are grateful to the 973 program 2013CB632300, Gansu Provincial Youth Science and Technology Fund Program (Grant no. 1606RJYA223), and the National Natural Science Foundation of China (Grant no. 51275508, 51305434) for financial support. They also wish to thank especially Dr Fuguo Wang and Kaixiong Gao for providing the samples. The help rendered by the other students in the sample testing and other aspects is also gratefully acknowledged.

References

[1] A. Modabberasl, P. Kameli, M. Ranjbar, H. Salamati, R. Ashiri, *Carbon*, **2015**, *94*, 485–493.
[2] X. Liu, J. Yang, J. Hao, J. Zheng, Q. Gong, W. Liu, *Adv. Mater.*, **2012**, *24*, 4614–4617.
[3] A. Erdemir, C. Donnet, *J. Phys. D Appl. Phys.*, **2006**, *39*, R311–R327.
[4] A. Erdemir, *Tribol. Int.*, **2004**, *37*, 1005–1012.
[5] L. C. Cui, Z. B. Lu, L. P. Wang, *ACS Appl. Mater. Interfaces*, **2013**, *5*, 5889–5893.
[6] A. Erdemir, *Surf. Coat. Technol.*, **2001**, *146*, 292–297.
[7] H. X. Li, T. Xu, C. B. Wang, J. M. Chen, H. D. Zhou, H. W. Liu, *Tribol. Int.*, **2007**, *40*, 132–138.
[8] C. Donnet, J. Fontaine, A. Grill, T. L. Mogne, *Tribol. Lett.*, **2000**, *9*, 137–142.
[9] O. L. Eryilmaz, A. Erdemir, *Surf. Coat. Technol.*, **2007**, *201*, 7401–7407.
[10] Z. Q. Yao, P. Yang, N. Huang, H. Sun, J. Wang, *Appl. Surf. Sci.*, **2004**, *230*, 172–178.
[11] F. G. Sen, Y. Qi, A. T. Alpas, *J. Mater. Res.*, **2009**, *24*, 2461–2470.
[12] F. G. Sen, Y. Qi, A. T. Alpas, *Acta Mater.*, **2011**, *59*, 2601–2614.
[13] F. G. Sen, Y. Qi, A. T. Alpas, *Lubr. Sci.*, **2013**, *25*, 111–121.
[14] I. Elgayar, A. E. Aliev, A. R. Boccaccini, R. G. Hill, *J. Non Cryst. Solids*, **2005**, *351*, 173–183.
[15] W. Zhang, J. R. Smith, *Phys. Rev. B*, **2000**, *61*, 16883–16889.
[16] R. Di Felice, J. E. Northrup, *Phys. Rev. B*, **1999**, *60*, 16287–16290.
[17] A. C. Ferrari, J. Robertson, *Phys. Rev. B*, **2000**, *61*, 14095–14107.
[18] G. Irmer, A. Dorner-Reisel, *Adv. Eng. Mater.*, **2005**, *7*, 694–705.
[19] A. H. Jiang, J. R. Xiao, X. Y. Li, Z. Y. Wang, *J. Nanomater.*, **2013**, *2013*, 15158–15166.
[20] M. F. Jiang, Z. Y. Ning, *J. Non Cryst. Solids*, **2005**, *351*, 2462–2467.
[21] X. X. Ma, G. Z. Tang, M. R. Sun, *Surf. Coat. Technol.*, **2007**, *201*, 7641–7644.
[22] J. C. Sung, M. C. Kan, M. Sung, *Int. J. Refract. Met. Hard Mater.*, **2009**, *27*, 421–426.
[23] J. J. Wang, F. Wang, J. M. Li, Q. Sun, P. F. Yuan, Y. Jia, *Surf. Sci.*, **2013**, *608*, 74–79.

